CHEMISTRY
A European Journal

A Journal of
ChemPubSoc Europe

## Accepted Article

**Title:** Kinetic Control of Self-Assembly Pathway towards Hidden Chiral Microcoils

**Authors:** Yongxian Guo, Yin Liu, Yanjun Gong, Wei Xiong, Chuang Zhang, Jincai Zhao, and Yanke Che



**To be cited as:** *Chem. Eur. J.* 10.1002/chem.201901120

**Link to VoR:** http://dx.doi.org/10.1002/chem.201901120

Supported by
ACES

WILEY-VCH

10.1002/chem.201901120

WILEY-VCH

COMMUNICATION

# Kinetic Control of Self-Assembly Pathway towards Hidden Chiral Microcoils

Yongxian Guo,[#] Yin Liu,[#] Yanjun Gong, Wei Xiong, Chuang Zhang,* Jincai Zhao and Yanke Che*

**Abstract:** Manipulating the self-assembly pathway is essentially important in the supramolecular synthesis of organic nano- and micro-architectures. Here we design a series of photoisomerizable chiral molecules, and realize the precise control over pathway complexity with external light stimuli. The hidden single-handed microcoils, rather than the straight microribbons via spontaneous assembly, are obtained through the kinetics-controlled pathway. The competition between molecular interactions in metastable photostationary intermediates gives rise to the variety of molecular packing and thereby the possibility of chirality transfer from molecules to supramolecular assemblies.

Analogous to the formation and growth processes of protein fibrils,[1-2] pathway complexity has been discovered to involve in the self-assembly process of many synthetic systems.[3-33] Furthermore, pathway complexity has been proven to be critical to achieve kinetically stable micro-/nano-architectures[8-16]and to yield a living supramolecular polymerization.[13,22-33] For example, Meijer and coworkers have selectively obtained the metastable assemblies based on the systematical studies on the kinetics-controlled pathway complexity.[8-9,12,17] Takeuchi et al. have first reported the use of pathway complexity in the design and realization of living supramolecular polymerization.[25] Despite the many advances on pathway complexity in the supramolecular self-assembly, facile and precise control over the pathways toward specific assembly structures remains a great challenge in practice. This is mainly because different pathways often proceed concurrently and tangle together, thereby hindering the selective synthesis of desired architectures. In addition, some of the kinetically stable assemblies are deeply trapped in the energy landscape and the thermodynamically stable assembly may not be accessed.[8-11, 24]

In this work, we report the pathway complexity in the self-assembly of photoisomerizable chiral molecule **1** (Figure 1a), and fabricate the hidden single-handed microcoils through a kinetics-controlled pathway triggered by photoirradiation. We reveal that the photoirradiation at the initial self-assembly stage can photoisomerize *trans*-**1** into *cis*-**1** molecules, which firstly form metastable aggregates, then slowly disassemble and isomerize back into *trans*-**1** monomers. Importantly, this kinetics-controlled pathway leads to the nucleation and elongation of single-handed microcoils (Pathway B, Figure 1b), which is in sharp contrast to the spontaneous self-assembly pathway towards the instant formation of straight microribbons (Pathway A, Figure 1b). Structural and optical characterizations show that the pathway complexity originates from the molecular interaction competition and gives rise to various supramolecular assemblies. Here, our finding, i.e., using a kinetics-controlled pathway to introduce extra molecular interaction for the formation of hidden chiral microcoils, provides a new example of utilizing the pathway complexity for novel functional supramolecular materials.

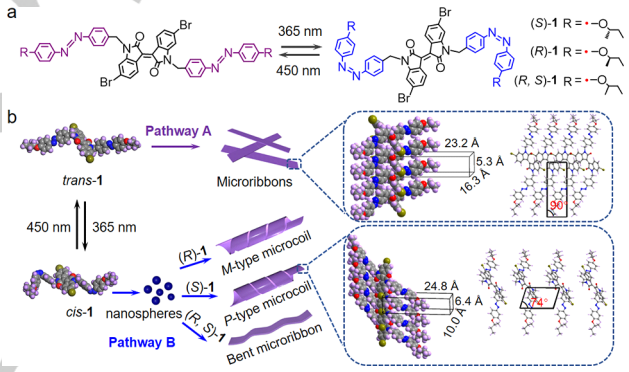


**Figure 1.** (a) Molecular structures of molecule **1** and the reversible transformation between *trans* and *cis* conformations induced by UV/visible light irradiation. (b) Schematic illustration of pathway complexity in the self-assembly of molecule **1**, including the formation of microribbons by a spontaneous self-assembly pathway (Pathway A), the formation of single-handed microcoils of chiral molecular **1** and the formation of bent microribbons of racemic (*R, S*)-**1** by photo-initiated self-assembly pathways (Pathway B). The images in dashed frames are the lattice parameters and internal organization of microribbons and microcoils, respectively.

As shown in Figure 1a, chiral molecules, (*S*)-**1**, (*R*)-**1**, and racemic molecule (*R, S*)-**1** that bear indigo and azobenzene moieties were designed and synthesized (see Supporting Information, Scheme S1, Figure S1 to S8 for details), and their pathway complexity of self-assembly under photoirradiation was investigated. Given the reversible photoisomerization of azobenzene moieties in **1** that can create distinct intermolecular interactions, the photoregulated self-assembly property of **1** is expected. Furthermore, by modulating the photoisomerization extent and rate of **1** with light irradiation, the precise control on the concentration of *trans*-/*cis*-monomers can be achieved, analogues to other systems.[34-35] Before exploring the pathway complexity, we characterized the photoisomerization behaviors of molecularly dissolved *trans*-**1** by measuring its absorption spectra (Figure S9) in solution upon UV

[*] Y. Guo, Y. Liu, Y. Gong, W. Xiong, Prof. Dr. C. Zhang, Prof. Dr. J. Zhao, Prof. Dr. Y. Che
Key Laboratory of Photochemistry, CAS Research/Education Center for Excellence in Molecular Sciences, Institute of Chemistry, Chinese Academy of Sciences, Beijing 100190, China
and
University of Chinese Academy of Sciences, Beijing 100049, China
E-mail: zhangc@iccas.ac.cn; ykche@iccas.ac.cn
[#] These authors contributed equally to this work.

Supporting information for this article is given via a link at the end of the document.

10.1002/chem.201901120




irradiation (350-380 nm). During the 10 min irradiation, the π-π* absorption of *trans*-**1** around 360 nm gradually decreased, while the absorption band centered at ca. 450 nm corresponding to the n-π* transition of *cis*-**1** increased. This result indicates that the *trans* to *cis* photoisomerization occurred rapidly. The yielded ratio of *trans*-**1** to *cis*-**1** after UV radiation was quantified to be 20:80 according to the $^{1}$H NMR spectra of the photostationary product (Figure S10). The reaction rate of *cis*-**1** to *trans*-**1** isomerization is slow in the dark and the *cis*-**1** molecules exist for several hours (Figure S11). Visible light (420-700 nm) can increase the rate of reversion reaction by over 1000 times (Figure S12), thereby offering an alternative way to the kinetic control over the *trans*-/*cis*- monomer concentrations. Importantly, self-assembly of *trans*-**1** with kinetically controlled concentration serves as a new self-assembly pathway, thereby providing opportunities to construct assemblies with unusual microscale architectures.

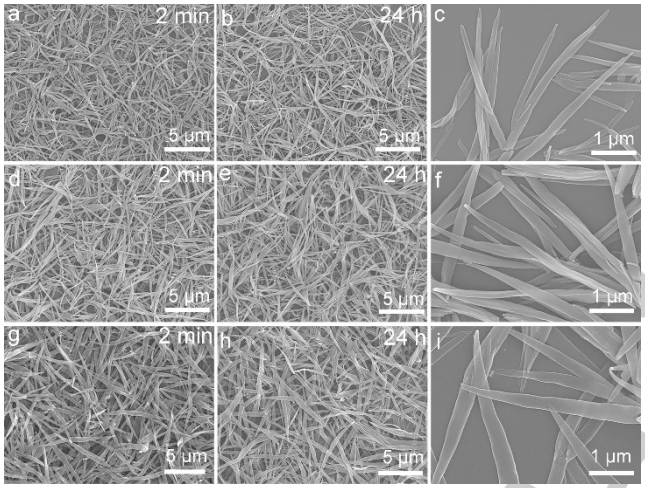


**Figure 2.** SEM images of microribbons assembled from *trans*-(*S*)-**1** (a-c), *trans*-(*R*)-**1** (d-f), and *trans*-(*R, S*)-**1** (g-i) at different time points: 2 min (a, d, g), 24 h (b, e, h), and amplified images (c, f, i).

We first used scanning electronic microscopy (SEM) to monitor the spontaneous self-assembly process of pure *trans*-**1** (Pathway A). As shown in Figure 2a-c, the ribbon-like structures with lengths of several micrometers were formed immediately after fully mixing 0.1 mL chloroform solution of *trans*-(*S*)-**1** ($4.2 \times 10^{-4}$ M) with 1.5 mL methanol as the poor solvent (see details in the Supporting Information). The morphology of resulting products remained unchanged even after 30 days (Figure S13), showing that these assemblies are thermodynamically stable structures. The crystal structure of these ribbons was analyzed by X-ray diffraction (XRD) and selected area electron diffraction (SAED) measurement, thereby the molecular packing of the ribbons can be simulated accordingly (Figure S14). A closer examination showed that the distance between neighboring indigo moieties is 3.55 Å, suggesting that the π-π interaction was the dominant driving force for the ribbon formation. Notably, *trans*-(*R*)-**1** and *trans*-(*R, S*)-**1** molecules also self-assembled into ribbon-like structures under the same self-assembly conditions (Figure 2d-i). XRD measurements (Figure S15) proved that the ribbons of *trans*-(*R*)-**1** and *trans*-(*R, S*)-**1** share the same molecular packing mode as those of *trans*-(*S*)-**1**, regardless of the opposite point chirality in the substituent. These results demonstrate that π-π interaction outcompetes other molecular interactions such as the chirality transfer, and dominates the fast nucleation-elongation of molecule **1** into ribbon structures.

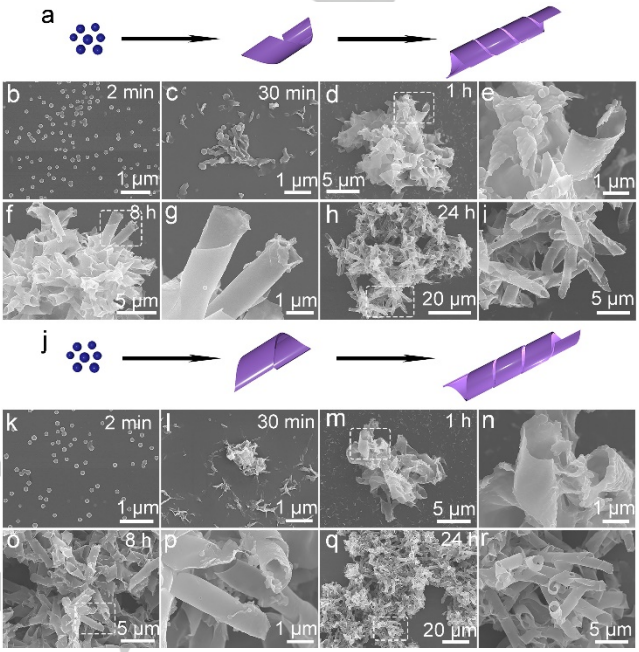


**Figure 3.** SEM images of the assembly evolution of (*S*)-**1** (a-i) and (*R*)-**1** (j-r) at different time points. (a) Schematic illustration of morphology evolution by photo-initiated self-assembly process of (*S*)-**1**. (b) Nanospheres formed at 2 min after adding the UV irradiated (*S*)-**1** monomer into methanol. (c) Microscale irregular aggregate formed at 30 min from the deformation of nanospheres. (d, e) Curved chiral nucleus formed at 1 h. (f, g) Nanospheres aggregates onto the termini of the tubular ribbons for epitaxial growth at 8h. (h, i) Single-handed microcoils formed at 24 h. (j-r) are the same as (a-i) but for (*R*)-**1**.

We next explored the kinetics-controlled self-assembly of *trans*-**1** (Pathway B), where the *trans*-**1** concentration in monomers depends on the kinetic reversion from *cis*-**1** to *trans*-**1**. In a typical self-assembly process, a chloroform solution (0.1 mL) of *trans*-(*S*)-**1** molecule ($4.2 \times 10^{-4}$ M) was firstly irradiated by 365 nm UV light (10 mW/cm$^2$) for 10 min to yield a mixture of *trans*-**1** and *cis*-**1** (20:80), and then injected into 1.5 mL methanol followed by stirring and aging in the dark. Interestingly, spherical nanoparticles with diameters ranging from 100 nm to 150 nm were formed at 2 min after the beginning the self-assembly process (Figure 3b and Figure S16). Then these nanospheres evolved into curved structures and bounded together (Figure 3c). At 1 h, well-defined cambered structures were observed (Figure 3d, e), indicative of the formation of new *trans*-(*S*)-**1** structural nuclei. As time progressed, the cambered nuclei continued to grow into microscale coiled structures (Figure 3f, g). A closer examination revealed that the microcoil ends were irregular at this stage, which were still accompanied with small curved structures and a small number of nanospheres (Figure 3g). After 24 h, only large *trans*-(*S*)-**1** microcoils with a diameter of ca. 2 μm and a length of ca. 10

10.1002/chem.201901120




μm were observed without the existence of small curved structures and nanospheres (Figure 3h, i and Figure S17).

The above observations suggest that the nanospheres intermediates slowly disassembled into monomers that could form cambered nuclei and grow into well-defined microcoils, analogous to the metastable aggregates involved in other supramolecular systems that mediate the nucleation and growth of stable structures.[25,27] The building blocks of the obtained microcoils are *trans*-**1** molecules revealed by measuring the absorption spectrum of microcoils suspension (Figure S18). Notably, the resulting microcoils are all single-handed (*P*-type) as revealed in magnified SEM images (Figure S19) and transmission electron microscopy (TEM) images (Figure S20). In accordance with the results of XRD and SAED, we simulated the molecular packing of *trans*-(*S*)-**1** and calculated the distance between indigo moieties in microcoils to be 3.84 Å (Figure S21). The larger intermolecular spacing compared with that in microribbons suggests the cooperative interactions among π-interaction, steric interaction, and chirality transfer dominantly drive the formation of microcoils.[36-38]

Likewise, the stepwise formation of microcoils from *trans*-(*R*)-**1** monomers was observed through the kinetics-controlled self-assembly Pathway B (Figure 3j-r). Instead, the resulting microcoils were *M*-type assemblies (Figure S22). XRD measurements confirmed a similar molecular packing (Figure S23) but in mirror image. These results indicate that the transfer of point chirality becomes critical in the interaction competition and gives rise to single-handed microcoils in the kinetics-controlled self-assembly pathway. This is in sharp contrast with the spontaneous self-assembly of pure *trans*-**1** monomer (Pathway A) where the transfer of point chirality was outcompeted by π-π interaction.

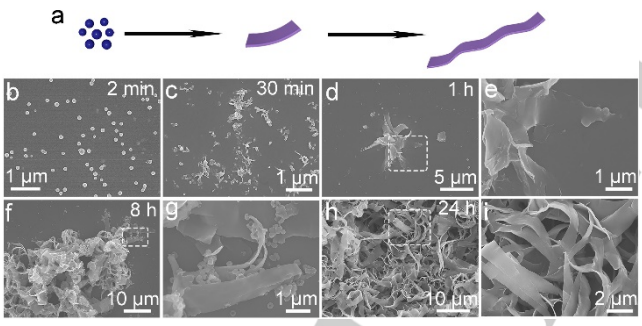


**Figure 4.** SEM images of the assembly evolution of (*R, S*)-**1** at different time points. (a) Schematic illustration of morphology evolution by the photo-initiated self-assembly of (*R, S*)-**1** molecules. (b) Nanospheres formed at 2 min after adding UV-irradiated (*R, S*)-**1** monomer into methanol. (c) Microscale curved aggregates formed at 30 min from the deformation of nanospheres. (d, e) Achiral nucleus formed at 1 h. (f, g) Nanospheres aggregate onto the termini of bent ribbons for epitaxial growth at 8 h. (h, i) Achiral bent microribbons formed at 24 h.

To further understand how the interaction competition leads to the morphological transition in Pathway B, we monitored the kinetics-controlled self-assembly of (*R, S*)-**1** (Figure 4a) that lacks the point chirality. Similar to (*S*)-**1** or (*R*)-**1**, chloroform solution (0.1 mL) of (*R, S*)-**1** molecule ($4.2 \times 10^{-4}$ M) was firstly irradiated by 365 nm UV light (10 mW/cm$^2$) for 10 min to yield *trans*-**1**:*cis*-**1**=20:80 monomers and then injected into 1.5 mL methanol followed by fully stirring and aging in the dark. At 2 min after beginning the self-assembly process, nanospheres was initially formed (Figure 4b), and then evolved into curved structures (Figure 4c). Unlike the case of (*S*)-**1** or (*R*)-**1**, these curved assemblies of (*R, S*)-**1** exhibited no preferential helicity (Figure 4d, e) and grew into randomly bent microribbons along with a decreasing number of nanospheres as time progressed (Figure 4f, g). After 24 h, only well-defined bent microribbons were observed, indicating that all metastable aggregates were disassembled for the microribbon growth. XRD and SAED patterns showed that the resulting bent microribbons (Figure S24) are different in crystal structures from those (*S*)-**1** or (*R*)-**1** microcoils, but consistent with the microribbons obtained by spontaneous self-assembly pathway (Figure S14). These observations illustrate that the chirality transfer of chiral **1** is necessary for the formation of single-handed coiled structures at the nucleation stage of kinetics-controlled self-assembly. The molecular interaction that drove the formation of nanospheres was also revealed by optical characterization. The absorption of nanospheres suspension obtained at 2 min (Figure S25) is similar to that of UV-irradiated monomer solution, showing that the building blocks of nanosphere are mainly *cis*- **1** molecules. This result indicates that the formation of metastable nanospheres was mainly driven by the steric repulsion among photogenerated *cis*-**1** molecules. We also performed XRD measurements of the metastable nanosphere assemblies. No XRD peaks were observed from the nanosphere aggregates due to their amorphous structural nature. After 1 h, XRD features of ordered molecular packing appeared (Figure S26), suggesting that the cooperative effect among π-π interaction, steric interaction, and chirality transfer (existing only for chiral **1**) began to mediate the nucleation of assemblies.

The kinetic reversion rate from *cis* to *trans* form can also influence on the interaction competition and consequently on the morphology of the resulting assemblies. We applied visible light irradiation (420-700 nm, 100 mW/cm$^2$) on metastable *cis*-**1** nanospheres to facilitate the formation of *trans*-**1**. As shown in Figure S27, straight microribbons with ca. 3 μm in width and ca. 40 μm in length were immediately formed after 5 min under visible irradiation. XRD measurements showed that these rapidly formed ribbons have the same molecular packing (Figure S28) as the ribbons from the spontaneous assembly of *trans*-**1** (Pathway A). Obviously, the concentration of *trans*-**1** monomer significantly increases under this condition, which allows π-π interaction to be the dominant driving force that leads to the formation of microribbons. This result further indicates that the formation of microcoils necessitates the kinetics-controlled self-assembly pathway with a proper interaction competition.

In conclusion, we present the self-assembly pathway complexity of molecule **1** that involves distinct competition of molecular interactions and thereby results in assemblies with diverse morphologies. Particularly, the fabrication of hidden single-handed microcoils is achieved through the kinetics-controlled self-assembly pathway, where the photoirradiation on chiral *trans*-**1** at the initial self-assembly stage introduces the morphological transition from metastable nanospheres to cambered nuclei and to single-handed microcoils. Our results prove the importance of

pathway complexity in achieving novel microscale architectures in the synthetic systems, and offer a photochemical method to manipulate self-assembly pathways towards precisely controlled synthesis of supramolecular assemblies.[39-42]

## Acknowledgements

This work was supported by the "National Key R&D Program of China" (No. 2018YFA0209302), the National Natural Science Foundation of China (Nos. 21577147, 21590811 and 21677148), and the "Key Research Program of Frontier Sciences" (No. QYZDY-SSW-SLH028) of the Chinese Academy of Sciences.

**Keywords:** Azobenzene • photoisomerization • Kinetic control • Pathway Complexity • Chirality

[1] A. M. Mulder, *Science* **2010**, *330*, 673-677.
[2] E. T. Powers, D. L. Powers, *Biophys. J.* **2008**, *94*, 379-391.
[3] J. M. A. Carnall, C. A. Waudby, A. M. Belenguer, M. C. A. Stuart, J. J.-P. Peyralans, S. Otto, *Science* **2010**, *327*, 1502-1506.
[4] D. V. D. Zwaag, P. A. Pieters, P. A. Korevaar, A. J. Markvoort, A. J. H. Spiering, T. F. A. D. Greef, , E. W. Meijer, *J. Am. Chem. Soc.* **2015**, *137*, 12677-12688.
[5] S. Ogi, T. Fukui, J. Melinda L, M. Takeuchi, K. Sugiyasu, *Angew. Chem. Int. Ed.* **2014**, *53*, 14363-14367; *Angew. Chem.* **2014**, *126*, 14591-14595.
[6] E. E. Greciano, B. Matarranz, n. L. Sanchez, *Angew. Chem. Int. Ed.* **2018**, *57*, 4697-4701; *Angew.Chem.* **2018**, *130*, 4787-4791.
[7] J. W. Sadownik, E. Mattia, P. Nowak, S. Otto, *Nat. Chem.* **2016**, *8*, 264-269.
[8] P. A. Korevaar, S. J. George, A. J. Markvoort, M. M. J. Smulders, P. A. J. Hilbers, A. P. H. J. Schenning, T. F. A. D. Greef, E. W. Meijer, *Nature* **2012**, *481*, 492-496.
[9] A. T. Haedler, S. C. J. Meskers, R. H. Zha, M. Kivala, H. W. Schmidt, E. W. Meijer, *J. Am. Chem. Soc.* **2016**, *138*, 10539-10545.
[10] F. Tantakitti, J. Boekhoven, X. Wang, R. V. Kazantsev, T. Yu, J. Li, E. Zhuang, R. Zandi, J. H. Ortony, C. J. Newcomb, L. C. Palmer, G. S. Shekhawat, M. O. de la Cruz, G. C. Schatz, S. I. Stupp, *Nat. Mater.* **2016**, *15*, 469-476.
[11] Y. Zhang, Y. Zheng, W. Xiong, C. Peng, Y. Zhang, R. Duan, Y. Che, J. Zhao, *Sci. Rep.* **2016**, *6*, 27335.
[12] P. A. Korevaar, C. J. Newcomb, E. W. Meijer, S. I. Stupp, *J. Am. Chem. Soc.* **2014**, *136*, 8540-8543.
[13] A. Aliprandi, M. Mauro, L. D. Cola, *Nat. Chem.* **2016**, *8*, 10-15.
[14] B. Kemper, L. Zengerling, D. Spitzer, R. Otter, T. Bauer, P. Besenius, *J. Am. Chem. Soc.* **2018**, *140*, 534-537.
[15] J. S. Valera, R. Gómez, L. Sanchez, *Angew. Chem. Int. Ed.* **2019**, *58*, 510-514; *Angew.Chem.* **2019**, *131*,520–524.
[16] Y. Wang, R. M. de Kruijff, M. Lovrak, X. Guo, R. Eelkema, J. H. van Esch, *Angew. Chem. Int. Ed.* **2019**, 58, 3800-3803; *Angew. Chem.* **2019**, 131, 3840-3843.
[17] M. F. J. Mabesoone, A. J. Markvoort, M. Banno, T. Yamaguchi, F. Helmich, Y. Naito, E. Yashima, A. R. A. Palmans, E. W. Meijer, *J. Am. Chem. Soc.* **2018**, *140*, 7810-7819.
[18] S. Ogi, V. Stepanenko, J. Thein, F. Würthner, *J. Am. Chem. Soc.* **2016**, *138*, 670-678.
[19] X. Ma, Y. Zhang, Y. Zhang, C. Peng, Y. Che, J. Zhao, *Adv. Mater.* **2015**, *27*, 7746-7751.
[20] S. Matsubara, H. Tamiaki, *J. Am. Chem. Soc.* **2019**, *141*, 1207-1211.
[21] P. Xing, P. Li, H. Chen, A. Hao, Y. Zhao, *Acs Nano* **2017**, *11*, 4206-4216.
[22] J. S. Valera, R. GoMez, L. Sanchez, *Small* **2018**, *14*, 1702437.
[23] S. Ogi, C. Grzeszkiewicz, F. Würthner, *Chem. Sci.* **2018**, *9*, 2768-2773.
[24] T. Fukui, S. Kawai, S. Fujinuma, Y. Matsushita, T. Yasuda, T. Sakurai, S. Seki, M. Takeuchi, K. Sugiyasu, *Nat. Chem.* **2017**, *9*, 493-499.
[25] S. Ogi, K. Sugiyasu, S. Manna, S. Samitsu, M. Takeuchi, *Nat. Chem.* **2014**, *6*, 188-195.
[26] M. Endo, T. Fukui, S. H. Jung, S. Yagai, M. Takeuchi, K. Sugiyasu, *J. Am. Chem. Soc.* **2016**, *138*, 14347-14353.
[27] X. Ma, Y. Zhang, Y. Zhang, Y. Liu, Y. Che, J. Zhao, *Angew. Chem. Int. Ed.* **2016**, *55*, 9539-9543; *Angew. Chem.* **2016**, *128*, 9691-9695.
[28] Y. Liu, C. Peng, W. Xiong, Y. Zhang, Y. Gong, Y. Che, J. Zhao, *Angew. Chem. Int. Ed.* **2017**, *56*, 11380-11384; *Angew. Chem.* **2017**, *129*, 11538-11542.
[29] M. E. Robinson, A. Nazemi, D. J. Lunn, D. W. Hayward, C. E. Boott, M. S. Hsiao, R. L. Harniman, S. A. Davis, G. R. Whittell, R. M. Richardson, L. D. Cola, I. Manners, *Acs Nano* **2017**, *11*, 9162-9175.
[30] M. E. Robinson, D. J. Lunn, A. Nazemi, G. R. Whittell, L. D. Cola, I. Manners, *Chem. Comm.* **2015**, *51*, 15921-15924.
[31] S. Ogi, K. Matsumoto, S. Yamaguchi, *Angew. Chem. Int. Ed.* **2018**, *57*, 2339-2343; *Angew. Chem.* **2018**, *130*, 2363-2367.
[32] S. Ogi, V. Stepanenko, K. Sugiyasu, M. Takeuchi, F. Würthner, *J. Am. Chem. Soc.* **2015**, *137*, 3300-3307.
[33] J. Boekhoven, J. M. Poolman, C. Maity, F. Li, L. van der Mee, C. B. Minkenberg, E. Mendes, J. H. van Esch, R. Eelkema, *Nat. Chem.* **2013**, *5*, 433-437.
[34] C. E. Weston, R. D. Richardson, P. R. Haycock, A. J. P. White, M. J. Fuchter, *J. Am. Chem. Soc.* **2014**, *136*, 11878-11881.
[35] J. Calbo, C. E. Weston, A. J. P. White, H. S. Rzepa, J. Contreras-García, M. J. Fuchter, *J. Am. Chem. Soc.* **2017**, *139*, 1261-1274.
[36] I. Danila, F. Riobe, F. Piron, J. Puigmarti-Luis, J. D. Wallis, M. Linares, H. Agren, D. Beljonne, D. B. Amabilino, N. Avarvari, *J. Am. Chem. Soc.* **2011**, *133*, 8344-8353.
[37] W. Zhang, W. Jin, T. Fukushima, N. Ishii, T. Aida, *J. Am. Chem. Soc.* **2013**, *135*, 114-117.
[38] W. Zhang, W. Jin, T. Fukushima, T. Mori, T. Aida, *J. Am. Chem. Soc.* **2015**, *137*, 13792-13795.
[39] I. Danila, F. Pop, C. Escudero, L. N. Feldborg, J. Puigmarti-Luis, F. Riobe, N. Avarvari, D. B. Amabilino, *Chem. Commun.* **2012**, *48*, 4552-4554.
[40] F. Pop, C. Melan, I. Danila, M. Linares, D. Beljonne, D. B. Amabilino, N. Avarvari, *Chem. Eur. J.* **2014**, *20*, 17443-17453.
[41] L. Zhang, T. Wang, Z. Shen, M. Liu, *Adv. Mater.* **2016**, *28*, 1044-1059.
[42] J. Jiang, Y. Meng, L. Zhang, M. Liu, *J. Am. Chem. Soc.* **2016**, *138,* 15629-15635.

10.1002/chem.201901120

WILEY-VCH



**Entry for the Table of Contents**

# COMMUNICATION

Pathway complexity achieved by chiral molecule **1**, which obtained chiral expressed single-handed microcoils by photo-initiated kinetic controlled self-assembly pathway B, ribbon-like architectures obtained by spontaneous self-assembly pathway A without chiral expression. Distinct competition of molecular interactions among π-π interaction, steric interaction, and chirality transfer is the mainspring of the pathway differentiation.

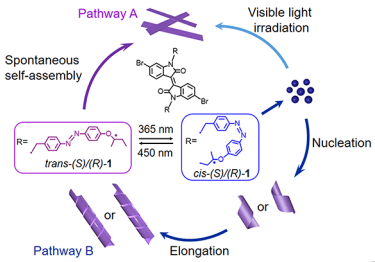


*Yongxian Guo,[#] Yin Liu,[#] Yanjun Gong, Wei Xiong, Chuang Zhang,* Jincai Zhao and Yanke Che**

***Page No. – Page No.***

**Kinetic Control of Self-Assembly Pathway towards Hidden Chiral Microcoils**